

---

# Fluctuation Pressure of a Stack of Membranes

---

We calculate the universal constants  $\alpha_N$  in Helfrich's pressure law for a stack of  $N$  membranes between walls by strong-coupling theory [49]. Using the close analogy between this system and a stack of strings, where the universal constants are exactly known, we construct a smooth potential that keeps the membranes apart. The strong-coupling limit of the perturbative treatment of the free energy yields pressure constants for an arbitrary number of membranes, which are in very good agreement with values from Monte Carlo simulations.

## 12.1 Introduction

The tension of membranes vanishes in equilibrium with a reservoir of molecules. Its shape is governed by the extrinsic curvature energy  $E_C$ . If a stack of membranes is placed between two parallel walls, violent thermal out-of-plane fluctuations of the membranes exert a pressure  $p$  upon the walls. The pressure law is given by Eq. (10.1). The pressure constant for a single membrane,  $\alpha_1$ , was roughly estimated by theoretical [50] and Monte Carlo methods [85–88]. The most precise theoretical result was obtained by strong-coupling theory [48] (see also Chapter 11 of this thesis), yielding  $\alpha_1^{\text{th}} = 0.0797149$ , which lies well within the error bounds of the latest Monte Carlo estimate  $\alpha_1^{\text{MC}} = 0.0798 \pm 0.0003$  [88].

For more than one membrane between the walls, the strong-coupling calculation of Refs. [48,89] must be modified in a nontrivial way. We must find a different potential that keeps the membranes apart and whose strong-coupling limit ensures non-interpenetration. For this, we take advantage of the fact that membranes between walls have similar properties to a stack of nearly parallel strings fluctuating in a plane between line-like walls [98,99], in particular the same type of pressure law (10.1) with  $\kappa$  substituted by the string tension  $\sigma$ . The characteristic universal constants of the latter system were *exactly* calculated in Refs. [88,98] from an analogy to a gas of fermions in  $1+1$  dimensions [100–102]. We use these exact values to determine a potential that, when applied to the stack of membranes, yields a perturbation expansion for the pressure constants for an *arbitrary* number of membranes to be evaluated in the strong-coupling limit of complete repulsion.

Our results are in excellent agreement with all available Monte Carlo estimates [86–88] for  $N = 1, 3, 5$ . Extrapolating to  $N \rightarrow \infty$ , we estimate the pressure constant  $\alpha_\infty$  for infinitely many membranes.

## 12.2 Stack of Strings

We begin by studying the exactly solvable statistical properties of a stack of  $N$  almost parallel strings in a plane, which are not allowed to cross each other and whose average spacing at low temperature is  $a$ . The system is enclosed between parallel line-like walls with a separation  $L$  as illustrated in Fig. 12.1. In the Monge parameterization, the vertical position of a point of the  $n$ th string is  $z_n = z_n(x)$ . Since the vertical positions of the  $n$ th string are fluctuating around the low-temperature equilibrium position at  $na$ , it is useful to introduce the displacement fields

$$\varphi_n(x) \equiv z_n(x) - na. \quad (12.1)$$

The thermodynamic partition function is given by the functional integral

$$Z^s = \prod_{n=1}^N \prod_x \left[ \int_{\varphi_{n-1}(x)-a}^{\varphi_{n+1}(x)+a} \frac{d\varphi_n(x)}{\sqrt{2\pi k_B T/\sigma}} \right] \exp \left\{ -\frac{\sigma}{2k_B T} \sum_{n=1}^N \int_{-\infty}^{\infty} dx \left[ \frac{d\varphi_n(x)}{dx} \right]^2 \right\}, \quad (12.2)$$

where  $\sigma$  is the string tension,  $T$  is the temperature, and  $k_B$  is the Boltzmann factor. We are interested in the free energy per unit length

$$f_N^s \equiv -\frac{k_B T}{A} \ln Z^s, \quad (12.3)$$

with  $A = \int_{-\infty}^{\infty} dx$ . Since the strings may not pass through each other, the fluctuations  $\varphi_n(x)$  of the  $n$ th string are restricted to the interval

$$\varphi_n(x) \in \{\varphi_{n-1}(x) - a, \varphi_{n+1}(x) + a\}. \quad (12.4)$$

### 12.2.1 Free Fermion Model

The restriction (12.4) makes it difficult to solve the functional integral (12.2) explicitly. It is, however, possible to find a solution by identifying the system with a  $(1+1)$ -dimensional Fermi gas, as done by de Gennes [100]. Using this analogy, Gompper and Kroll [88] determined the  $1/a^2$  contribution to  $\Delta f_N^s$  relevant for the pressure law (10.1) as

$$\Delta f_N^s = \alpha_N^s \frac{(k_B T)^2}{\sigma a^2}, \quad (12.5)$$

with the pressure constants

$$\alpha_N^s = \frac{\pi^2}{12} \frac{2N+1}{N+1}. \quad (12.6)$$

For  $N \rightarrow \infty$ , this constant has the finite limit  $\alpha_\infty^s = \pi^2/6$ . The analogy with fermions cannot be used to calculate the free energy of a stack of membranes, where only approximate methods are available. We will tackle this problem by making use of a strong-coupling theory as in Refs. [48,89]. As a preparation, we apply this theory to the exactly solvable system of a stack of strings.

### 12.2.2 Perturbative Approach

The difficulty in solving the functional integral (12.2) arises from the restriction (12.4) of the fluctuations by the neighboring strings. To deal with this strong repulsion, we introduce into the action of the functional integral (12.2) a smooth potential that keeps the strings apart in such a way that the integration interval for the fluctuations can be extended to  $\varphi_n(x) \in \{-\infty, \infty\}$ . At the end, we take a strong-coupling limit, which ensures (12.4). In Refs. [48,89], such a method was used to evaluate the pressure constant for one membrane between walls. The smooth potential for the analogous case of

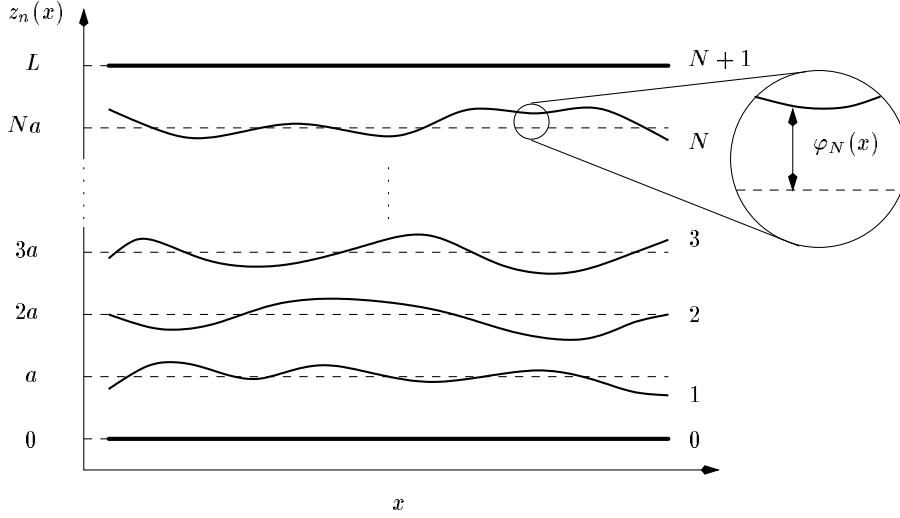


FIGURE 12.1: Stack of  $N$  strings with equilibrium spacing  $a$  between two walls of distance  $L$ . The magnifier shows the local displacement field  $\varphi_N(x)$  as the distance from the position  $Na$ . The walls are labeled by 0 and  $N+1$  and treated as non-fluctuating strings with  $\varphi_0(x) \equiv \varphi_{N+1}(x) \equiv 0$ .

one string is  $V(\varphi(x)) = (2a\mu/\pi)^2 \tan^2[\pi\varphi(x)/2a]$ , which describes the hard walls *exactly* for  $\mu \rightarrow 0$ . This potential is symmetric and possesses a minimum at  $\varphi(x) = 0$ . Thus its Taylor expansion around this minimum is a series in even powers of  $\varphi(x)$ .

In the case of  $N$  strings, the minima of the repulsion potential should lie at the equilibrium positions of the strings. The Taylor expansion of such a potential will also have terms with odd powers. Unlike the one-string system, where fluctuations are limited by fixed walls, the range of the displacements  $\varphi_n(x)$  of the  $n$ th string in an  $N$ -string system depends on the positions  $z_{n-1}(x)$  and  $z_{n+1}(x)$  of the neighboring strings. Thus the potential will be taken as a sum,

$$V_{\text{eff}}(z_0(x), z_1(x), \dots, z_N(x), z_{N+1}(x)) = \frac{\sigma}{2} \sum_{n=1}^{N+1} V_\mu(\bar{\nabla}_n z_n(x)), \quad (12.7)$$

where  $\bar{\nabla}_n z_n(x)$  denotes the prepoint lattice gradient  $z_n(x) - z_{n-1}(x)$ . This potential includes the interaction of the first and last strings with the walls as non-fluctuating strings at  $z_0 = 0$  and  $z_{N+1} = (N+1)a = L$ :

$$\varphi_0(x) = \varphi_{N+1}(x) = 0. \quad (12.8)$$

In the limit  $\mu \rightarrow 0$ , the potential  $V_\mu(\bar{\nabla}_n z_n(x))$  should again yield an infinitely strong repulsion of two neighboring strings for  $z_n(x)$  close to  $z_{n-1}(x)$ . For  $z_n(x) > z_{n-1}(x)$ , the limiting potential should be zero. As a matter of choice, we let the potential between two strings  $V_\mu(\bar{\nabla}_n z_n(x))$  be minimal and zero at the positions  $z_n^{\text{eq}} = na$  and  $z_{n-1}^{\text{eq}} = a(n-1)$ :  $dV_\mu(a)/d\bar{\nabla}_n z_n(x) = 0$  and  $V_\mu(z_n^{\text{eq}} - z_{n-1}^{\text{eq}}) = V_\mu(a) = 0$  (see Fig. 12.2).

The Taylor expansion around the minimum is, in terms of the variables (12.1),

$$V_\mu(\bar{\nabla}_n \varphi_n(x)) = \frac{\mu^2}{2} [\bar{\nabla}_n \varphi_n(x)]^2 + \mu^2 \sum_{k=1}^{\infty} c_k g^k [\bar{\nabla}_n \varphi_n(x)]^{k+2}. \quad (12.9)$$

The parameter  $\mu$  governs the harmonic term, whereas higher-order terms scale with the coupling constant  $g = 1/a$ , which makes the coefficients  $c_k$  dimensionless.

An example for a potential showing qualitatively the behavior in Fig. 12.2 with a Taylor expansion of the type (12.9) is  $V_\mu(\bar{\nabla}_n z_n(x)) = \mu^2 (a/[\bar{\nabla}_n z_n(x)]^2 - 2/\bar{\nabla}_n z_n(x) + 1/a)/2$ , which vanishes everywhere

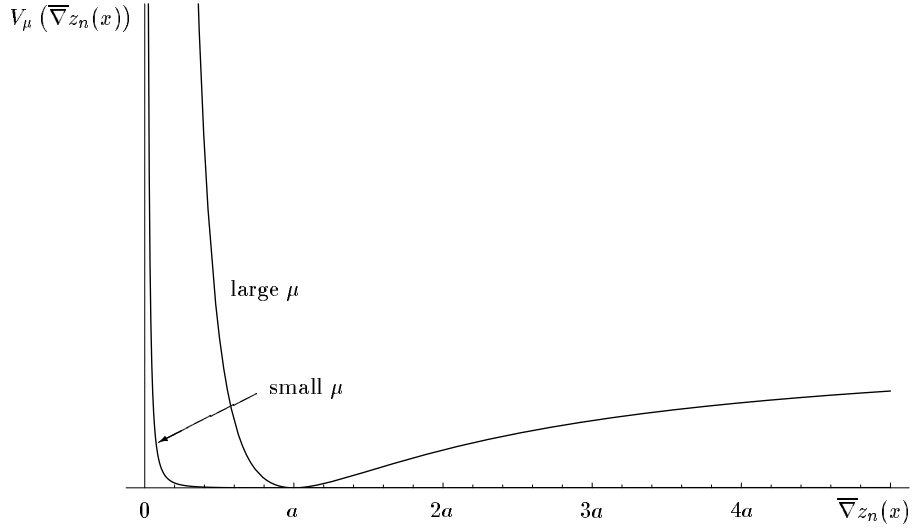


FIGURE 12.2: Potential  $V_\mu(\overline{\nabla}_n z_n(x))$  of string-string interaction for finite  $\mu$  and small  $\mu$  as a function of  $\overline{\nabla}_n z_n(x) = z_n(x) - z_{n-1}(x)$ . The strings repel each other strongly for  $\overline{\nabla}_n z_n(x) \rightarrow 0$ , while the potential has a minimum at the equilibrium separation  $\overline{\nabla}_n z_n(x) = a$ , and we choose to normalize it to zero at that point.

for infinitesimal  $\mu$ , except at  $\overline{\nabla}_n z_n(x) = 0$ . The strong-coupling limit of the perturbative expansion of order  $g^2$  presented in this chapter cannot yield, however, reasonable results for such an arbitrary choice of the potential. The calculation of higher-order perturbative coefficients requires high numerical power, which would make this procedure of calculating the universal constants inefficient.

Thus, we continue with the Taylor expansion (12.9), and the partition function (12.2) becomes

$$Z^s = \lim_{\mu \rightarrow 0} \oint \mathcal{D}^N \varphi(x) \exp \left\{ -\frac{\sigma}{2k_B T} \sum_{n=1}^{N+1} \int_{-\infty}^{\infty} dx \left( \left[ \frac{d\varphi_n(x)}{dx} \right]^2 + \frac{1}{2} \mu^2 [\overline{\nabla}_n \varphi_n(x)]^2 \right) \right\} \\ \times \exp \left\{ -\frac{\sigma}{2k_B T} \mu^2 \sum_{k=1}^{\infty} c_k g^k \sum_{n=1}^{N+1} \int_{-\infty}^{\infty} dx [\overline{\nabla}_n \varphi_n(x)]^{k+2} \right\} \quad (12.10)$$

with the integral measure

$$\oint \mathcal{D}^N \varphi(x) = \prod_{n=1}^N \prod_x \left[ \int_{-\infty}^{\infty} \frac{d\varphi_n(x)}{\sqrt{2\pi k_B T / \sigma}} \right]. \quad (12.11)$$

The harmonic part of the partition function can be written as

$$Z_\mu^s = \oint \mathcal{D}^N \varphi(x) \exp \left\{ -\frac{1}{2} \sum_{n=1}^{N+1} \sum_{n'=1}^{N+1} \int_{-\infty}^{\infty} dx \int_{-\infty}^{\infty} dx' \varphi_n(x) [G_{nn'}^s(x, x')]^{-1} \varphi_{n'}(x') \right\} \quad (12.12)$$

with the functional matrix

$$[G_{nn'}^s(x, x')]^{-1} = -\frac{\sigma}{k_B T} \left( \frac{d^2}{dx^2} + \frac{1}{2} \mu^2 \overline{\nabla}_n \nabla_n \right) \delta(x - x') \delta_{nn'}. \quad (12.13)$$

Here  $\nabla_n \varphi_n(x) = \varphi_{n+1}(x) - \varphi_n(x)$  denotes the postpoint lattice gradient in the  $z$  direction, and  $\overline{\nabla}_n \nabla_n$  is the lattice version of the Laplace operator [4].

Let us now impose the vanishing of the fluctuations of the walls (12.8), corresponding to Dirichlet boundary conditions. For a finite number  $N$  of strings, the Kronecker symbol  $\delta_{nn'}$  in Eq. (12.13) has the Fourier representation

$$\delta_{nn'} = \frac{2}{N+1} \sum_{m=1}^N \sin \nu_m n a \sin \nu_m n' a \quad (12.14)$$

with wave numbers  $\nu_m = \pi m / (N+1)a$ . Thus the kernel  $[G_{nn'}^s(x, x')]^{-1}$  may be written in Fourier space as

$$[G_{nn'}^s(x, x')]^{-1} = \frac{2}{N+1} \sum_{m=1}^N \sin \nu_m n a \sin \nu_m n' a \int_{-\infty}^{\infty} \frac{dk}{2\pi} [G_m^s(k)]^{-1} e^{-ik(x-x')} \quad (12.15)$$

with the Fourier components

$$[G_m^s(k)]^{-1} = \frac{\sigma}{k_B T} [k^2 + 2\mu^2 \sin^2(\nu_m a/2)]. \quad (12.16)$$

Integrating over  $k$  in the spectral representation (12.15) leads immediately to the correlation function in configuration space,

$$G_{nn'}^s(x, x') = \frac{1}{\sqrt{2}(N+1)} \frac{k_B T}{\mu\sigma} \sum_{m=1}^N \frac{\sin \nu_m n a \sin \nu_m n' a}{\sin(\nu_m a/2)} e^{-\sqrt{2}\mu|x-x'| \sin(\nu_m a/2)}, \quad (12.17)$$

and to the harmonic partition function (12.12),

$$Z_\mu^s = \exp \left\{ -\frac{1}{2} \text{Tr} \ln [G^s]^{-1} \right\} = e^{-A f_{N,\mu}^s / k_B T}, \quad (12.18)$$

the exponent giving the free energy per length,

$$f_{N,\mu}^s = \mu \frac{k_B T}{2} \frac{\sin[\pi N/4(N+1)]}{\sin[\pi/4(N+1)]}, \quad (12.19)$$

which vanishes for  $\mu = 0$ .

The full partition function  $Z^s$  in Eq. (12.10) is now calculated perturbatively. We introduce harmonic expectation values

$$\langle \cdots \rangle_\mu^s = [Z_\mu^s]^{-1} \oint \mathcal{D}^N \varphi(x) \cdots \exp \left\{ -\frac{1}{2} \sum_{n=1}^{N+1} \sum_{n'=1}^{N+1} \int_{-\infty}^{\infty} dx \int_{-\infty}^{\infty} dx' \varphi_n(x) [G_{nn'}^s(x, x')]^{-1} \varphi_{n'}(x') \right\} \quad (12.20)$$

in terms of which the correlation function is given by

$$G_{nn'}^s(x, x') = \langle \varphi_n(x) \varphi_{n'}(x') \rangle_\mu^s. \quad (12.21)$$

The perturbation expansion contains the two-point correlation function of  $\bar{\nabla}_n \varphi_n(x)$ , which is given by

$$\langle \bar{\nabla}_n \varphi_n(x) \bar{\nabla}_{n'} \varphi_{n'}(x') \rangle_\mu^s = \bar{\nabla}_n \bar{\nabla}_{n'} G_{nn'}^s(x, x'). \quad (12.22)$$

We now expand the second exponential in Eq. (12.10) in powers of the coupling constant  $g$ . Harmonic expectation values with odd powers of  $\bar{\nabla}_n \varphi_n(x)$  do not contribute, and the expansion reads

$$Z^s = \lim_{\mu \rightarrow 0} Z_\mu^s \left[ 1 - g^2 \left( \frac{\sigma}{2k_B T} \mu^2 c_2 \sum_{n=1}^{N+1} \int_{-\infty}^{\infty} dx \langle [\bar{\nabla}_n \varphi_n(x)]^4 \rangle_\mu^s \right) \right]$$

$$- \frac{1}{2!} \frac{\sigma^2}{4k_B^2 T^2} \mu^4 c_1^2 \sum_{n,n'=1}^{N+1} \int_{-\infty}^{\infty} dx \int_{-\infty}^{\infty} dx' \langle [\bar{\nabla}_n \varphi_n(x)]^3 [\bar{\nabla}_{n'} \varphi_{n'}(x')]^3 \rangle_{\mu}^s + \dots \Big]. \quad (12.23)$$

In the sequel, we restrict ourselves to the terms of second order in  $g = 1/a$ , which contribute directly to the pressure law as in Eq. (12.5). The higher powers diverge for  $\mu \rightarrow 0$ , and in Refs. [48,89] it was shown how to calculate from them a finite strong-coupling limit. Here we shall ignore these terms for reasons to be explained shortly. Re-expressing the right-hand side of Eq. (12.23) as an exponential of a cumulant expansion, we obtain the free energy per length,

$$f_N^s = \lim_{\mu \rightarrow 0} g^2 \left( \frac{\sigma}{2k_B T} \mu^2 c_2 \sum_{n=1}^{N+1} \int_{-\infty}^{\infty} dx \langle [\bar{\nabla}_n \varphi_n(x)]^4 \rangle_{\mu,c}^s - \frac{1}{2!} \frac{\sigma^2}{4k_B^2 T^2} \mu^4 c_1^2 \sum_{n,n'=1}^{N+1} \int_{-\infty}^{\infty} dx \int_{-\infty}^{\infty} dx' \langle [\bar{\nabla}_n \varphi_n(x)]^3 [\bar{\nabla}_{n'} \varphi_{n'}(x')]^3 \rangle_{\mu,c}^s \right) + \dots \quad (12.24)$$

We have used that the free energy  $f_{N,\mu}^s$  of the harmonic system (12.19) vanishes in the limit  $\mu \rightarrow 0$ . The first cumulants are the expectations

$$\begin{aligned} \langle O_1(\bar{\nabla} \varphi_{n_1}(x_1)) \rangle_{\mu,c}^s &= \langle O_1(\bar{\nabla} \varphi_{n_1}(x_1)) \rangle_{\mu}^s \\ \langle O_1(\bar{\nabla} \varphi_{n_1}(x_1)) O_2(\bar{\nabla} \varphi_{n_2}(x_2)) \rangle_{\mu,c}^s &= \langle O_1(\bar{\nabla} \varphi_{n_1}(x_1)) O_2(\bar{\nabla} \varphi_{n_2}(x_2)) \rangle_{\mu}^s \\ &\quad - \langle O_1(\bar{\nabla} \varphi_{n_1}(x_1)) \rangle_{\mu}^s \langle O_2(\bar{\nabla} \varphi_{n_2}(x_2)) \rangle_{\mu}^s, \\ &\quad \vdots \end{aligned} \quad (12.25)$$

defined for any polynomial function  $O_i(\bar{\nabla} \varphi_{n_i}(x_i))$  of  $\bar{\nabla} \varphi_{n_i}(x_i)$ . Following Wick's rule, we expand the expectations into products of two-point correlation functions (12.22). The different terms are displayed with the help of Feynman diagrams, in which lines and vertices represent the correlation functions and interactions:

$$x_1, n_1 \text{ --- } x_2, n_2 \longrightarrow \langle \bar{\nabla}_{n_1} \varphi_{n_1}(x_1) \bar{\nabla}_{n_2} \varphi_{n_2}(x_2) \rangle_{\mu}^s, \quad (12.26)$$

$$\bullet \longrightarrow \sum_{n=1}^{N+1} \int_{-\infty}^{\infty} dx. \quad (12.27)$$


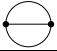

In what follows, we assume that the potential parameters  $c_k$  with  $k \geq 3$  are chosen in such a way that they make all terms of order  $g^3$  and higher vanish. Dividing the free energy (12.24) by  $N$ , we obtain the following expression for the free energy per length and string, which can be compared with Eq. (12.5):

$$\Delta f_N^s = \lim_{\mu \rightarrow 0} \left\{ \frac{3}{2} \frac{\sigma \mu^2}{A a^2} c_2 \text{ (diagram: two circles connected by a line)} - \frac{1}{8} \frac{\sigma^2 \mu^4}{k_B T A a^2} c_1^2 \left( 6 \text{ (diagram: circle with a line through it)} + 9 \text{ (diagram: two circles connected by a line)} \right) \right\}. \quad (12.28)$$

The calculation of the Feynman diagrams is straightforward using Eq. (12.17). The evaluation is only complicated by the Dirichlet boundary conditions, which destroy momentum conservation. This makes the numeric calculation quite time-consuming for an increasing number  $N$  of strings. As an explicit example, consider the sunset diagram, which requires the evaluation of the multiple sum

$$\begin{aligned} \text{(diagram: sunset)} &\equiv A \frac{k_B^3 T^3}{\mu^4} \frac{1}{2(N+1)^3} \sum_{n_1, n_2=1}^{N+1} \sum_{\substack{m_1, m_2, \\ m_3=1}}^N h_{n_1 n_2}^{m_1} h_{n_1 n_2}^{m_2} h_{n_1 n_2}^{m_3} \\ &\times \frac{1}{\sin(\nu_{m_1} a/2) \sin(\nu_{m_2} a/2) \sin(\nu_{m_3} a/2) [\sin(\nu_{m_1} a/2) + \sin(\nu_{m_2} a/2) + \sin(\nu_{m_3} a/2)]}, \end{aligned} \quad (12.29)$$

TABLE 12.1: Reduced numeric values  $W^{s,r}$  of the two-loop diagrams for the free energy for a stack of  $N$  strings.

$N$	 $^{s,r}$	 $^{s,r}$	 $^{s,r}$
1	1/2	0	0
2	1.288675	0.398717	0.089316
3	2.100656	0.832299	0.146447
4	2.915827	1.270787	0.184463
5	3.730993	1.709326	0.211325
6	4.545586	2.147034	0.231245
7	5.359574	2.583849	0.246583

with the abbreviation

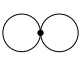
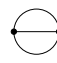
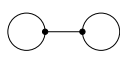
$$h_{n_1 n_2}^m = \sin \nu_m n_1 a \sin \nu_m n_2 a - \sin \nu_m n_1 a \sin \nu_m (n_2 - 1) a \\ - \sin \nu_m (n_1 - 1) a \sin \nu_m n_2 a + \sin \nu_m (n_1 - 1) a \sin \nu_m (n_2 - 1) a. \quad (12.30)$$

It is useful to factor out the physical dimension of the diagram. Any Feynman integral  $W^s$  with  $l$  lines and  $v$  vertices can be expressed in terms of a reduced dimensionless Feynman integral  $W^{s,r}$  as

$$W^s = A \left( \frac{k_B T}{\sigma} \right)^l \mu^{-(l+v-1)} W^{s,r}. \quad (12.31)$$

This brings Eq. (12.28) to the form

$$\Delta f_N^s = \alpha_N^s \frac{k_B^2 T^2}{\sigma a^2}, \quad (12.32)$$

$$\alpha_N^s = \frac{1}{N} \left[ \frac{3}{2} c_2 \text{   $^{s,r}$  - c_1^2 \left( \frac{3}{4} \text{   $^{s,r}$  + \frac{9}{8} \text{   $^{s,r}$  \right) \right], \quad (12.33)$$

where the diagrams indicate the reduced Feynman integrals. Their values are listed in Table 12.1 for different string numbers  $N$ . Note that the  $1/a^2$  contributions to the free energy per length and string in Eq. (12.28) are independent of  $\mu$  since the  $\mu$  prefactors are canceled by the  $\mu$  dependence of the diagrams. Thus the limit  $\mu \rightarrow 0$  becomes trivial for these contributions.

With the knowledge of the exact values of the constants  $\alpha_N^s$  from Eq. (12.6), we are now in a position to determine the potential parameters  $c_1$  and  $c_2$  from Eq. (12.33) to obtain the exact result from the two-loop expansion Eq. (12.33). Comparing Eqs. (12.33) and (12.6) for  $N = 1$  and  $N = 2$ , we obtain

$$c_1 = \frac{\pi}{3}, \quad c_2 = \frac{\pi^2}{6}. \quad (12.34)$$

Note that (12.33) consists of more equations than necessary to compute  $c_1$  and  $c_2$ . It turns out, however, that all of them give the same parameters  $c_1$  and  $c_2$ , such that the same potential (12.9) can be used for any  $N$ . This is the essential basis for applying this procedure to a stack of membranes.

We now justify the neglect of the higher  $g$  powers that would in principle give further contributions to the pressure constant  $\alpha_N^s$  in the strong-coupling limit. We simply observe that it is possible to choose the higher expansion coefficients  $c_k$  to make all higher  $g^n$  contributions vanish [103].

## 12.3 Stack of Membranes

Having determined the parameters  $c_1$  and  $c_2$  of the Taylor expansion (12.9) of the smooth potential applicable for any number of strings, we shall now use the same potential for a perturbative expansion in a stack of  $N$  membranes displayed in Fig. 12.3. The equilibrium spacing at low temperature between

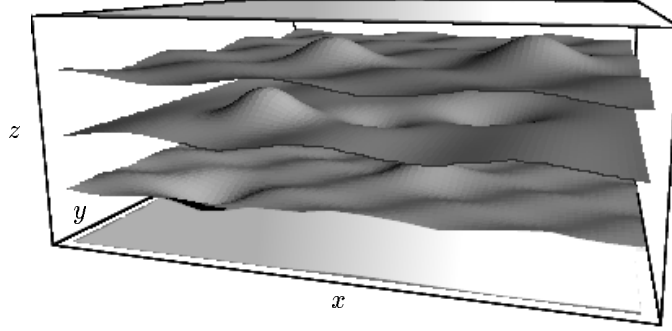


FIGURE 12.3: Stack of self-avoiding fluid membranes fluctuating in the  $z$  direction between two walls. As for the previous stack of strings, the walls are treated as non-fluctuating membranes.

the membranes is again  $a$ . Denoting the vectors in the plane by  $\mathbf{x} = (x, y)$ , the vertical displacements of the membranes from the positions  $na$  are  $\varphi_n(\mathbf{x})$ , with Dirichlet boundary conditions at  $z_0$  and  $z_{N+1}$ ,

$$\varphi_0(\mathbf{x}) = \varphi_{N+1}(\mathbf{x}) = 0. \quad (12.35)$$

For membranes without tension, the energy has the harmonic approximation

$$E_{C,n} = \frac{\kappa}{2} \int d^2x [\partial^2 \varphi_n(\mathbf{x})]^2, \quad (12.36)$$

where  $\kappa$  is the bending stiffness and  $\partial^2 = \partial_x^2 + \partial_y^2$  is the Laplacian in the plane parallel to the walls. By analogy with the preceding section, the kernel of the harmonic stack now reads

$$[G_{n_1 n_2}(\mathbf{x}_1, \mathbf{x}_2)]^{-1} = -\frac{\kappa}{k_B T} \left( [\partial_{\mathbf{x}_1}^2]^2 + \frac{1}{2} \mu^4 \bar{\nabla}_{n_1} \nabla_{n_1} \right) \delta(\mathbf{x}_1 - \mathbf{x}_2) \delta_{n_1 n_2}, \quad (12.37)$$

where we have used a mass parameter  $\mu^4$  instead of  $\mu^2$ , for dimensional reasons. The partition function for the stack of membranes is then written up to order  $g^2 = 1/a^2$  by

$$\begin{aligned} Z = & \lim_{\mu \rightarrow 0} \oint \mathcal{D}^N \varphi(\mathbf{x}) \exp \left\{ -\frac{1}{2} \sum_{n_1, n_2=1}^{N+1} \int d^2x_1 \int d^2x_2 \varphi_{n_1}(\mathbf{x}_1) [G_{n_1 n_2}(\mathbf{x}_1, \mathbf{x}_2)]^{-1} \varphi_{n_2}(\mathbf{x}_2) \right\} \\ & \times \left[ 1 - g^2 \left( \frac{\kappa}{2k_B T} \mu^4 c_2 \sum_{n=1}^{N+1} \int d^2x [\bar{\nabla} \varphi_n(\mathbf{x})]^4 - \frac{\kappa^2}{8k_B^2 T^2} \mu^8 c_1^2 \sum_{n_1, n_2=1}^{N+1} \int d^2x_1 \int d^2x_2 \right. \right. \\ & \left. \left. \times [\bar{\nabla} \varphi_{n_1}(\mathbf{x}_1)]^3 [\bar{\nabla} \varphi_{n_2}(\mathbf{x}_2)]^3 \right) \right], \quad (12.38) \end{aligned}$$

with the same parameters  $c_1$  and  $c_2$  of the Taylor expansion (12.9) as in the string system, determined in Eq. (12.34). We neglect terms of order  $g^3$ , which certainly contribute in the strong-coupling limit, and which vanish only for the strings, where the partition function (12.23) with the choice (12.34) for the parameters  $c_1, c_2$  is exact in second order. An evaluation of the neglected terms by variational perturbation theory is expected to give only a negligible contribution to our final result.

Inverting the kernel (12.37) yields the correlation function

$$G_{n_1 n_2}(\mathbf{x}_1, \mathbf{x}_2) = \frac{2}{N+1} \frac{k_B T}{\kappa} \sum_{m=1}^N \sin \nu_m n_1 a \sin \nu_m n_2 a \int \frac{d^2k}{(2\pi)^2} \frac{1}{k^4 + 2\mu^4 \sin^2(\nu_m a/2)} e^{-i\mathbf{k}(\mathbf{x}_1 - \mathbf{x}_2)}. \quad (12.39)$$



The explicit calculation of the Fourier integral leads to a difference of modified Bessel functions  $K_0(x)$  as in Ref. [48]:

$$G_{n_1 n_2}(\mathbf{x}_1, \mathbf{x}_2) = \frac{i}{\sqrt{8\pi(N+1)\mu^2}} \frac{k_B T}{\kappa} \sum_{m=1}^N \frac{\sin \nu_m n_1 a \sin \nu_m n_2 a}{\sin(\nu_m a/2)} \\ \times \left[ K_0 \left( 2^{1/4} \sqrt{i \sin(\nu_m a/2)} \mu |\mathbf{x}_1 - \mathbf{x}_2| \right) - K_0 \left( 2^{1/4} \sqrt{-i \sin(\nu_m a/2)} \mu |\mathbf{x}_1 - \mathbf{x}_2| \right) \right]. \quad (12.40)$$

For  $\mathbf{x}_1 = \mathbf{x}_2 \equiv \mathbf{x}$  and  $n_1 = n_2 \equiv n$ , this reduces to

$$G_{nn}(\mathbf{x}, \mathbf{x}) = \frac{1}{\sqrt{32}(N+1)\mu^2} \frac{k_B T}{\kappa} \sum_{m=1}^N \frac{\sin^2 \nu_m n a}{\sin(\nu_m a/2)}, \quad (12.41)$$

leading to the partition function of the harmonic system,

$$Z_\mu = \exp \left\{ -\frac{1}{2} \text{Tr} \ln G^{-1} \right\} = \exp \left\{ -\mu^2 \frac{A \sin[\pi N/4(N+1)]}{8 \sin[\pi/4(N+1)]} \right\}, \quad (12.42)$$

where  $A = \int d^2x$  is the area of the projected plane of the membranes. The free energy per area  $f_{N,\mu} = -(k_B T/A) \ln Z_\mu$  vanishes again for  $\mu = 0$ .

As for the calculation of the free energy of the stack of strings, we introduce harmonic expectation values

$$\langle \cdots \rangle_\mu = [Z_\mu]^{-1} \oint \mathcal{D}^N \varphi(\mathbf{x}) \cdots \exp \left\{ -\frac{1}{2} \sum_{n=1}^{N+1} \sum_{n'=1}^{N+1} \int_{-\infty}^{\infty} d^2x \int_{-\infty}^{\infty} d^2x' \varphi_n(\mathbf{x}) [G_{nn'}(\mathbf{x}, \mathbf{x}')]^{-1} \varphi_{n'}(\mathbf{x}') \right\}, \quad (12.43)$$

which appear in the perturbation expansion of Eq. (12.38), the cumulants yielding a perturbative expansion for the free energy per area  $f_N = -(k_B T/A) \ln Z$ . The lines and vertices in the Feynman diagrams now stand for

$$\mathbf{x}_1, n_1 \text{ --- } \mathbf{x}_2, n_2 \longrightarrow \langle \bar{\nabla}_{n_1} \varphi_{n_1}(\mathbf{x}_1) \bar{\nabla}_{n_2} \varphi_{n_2}(\mathbf{x}_2) \rangle_\mu \quad (12.44)$$

$$\bullet \longrightarrow \sum_{n=1}^{N+1} \int d^2x, \quad (12.45)$$

and the two-loop approximation to the free energy per area and membrane in order  $1/a^2$  reads

$$\Delta f_N = \lim_{\mu \rightarrow 0} \left\{ \frac{\pi^2 \kappa \mu^4}{4 A a^2} \text{---} \text{---} - \frac{\pi^2 \kappa^2 \mu^8}{k_B T A a^2} \left( \frac{1}{12} \text{---} \text{---} + \frac{1}{8} \text{---} \text{---} \right) \right\}. \quad (12.46)$$

Going over to reduced Feynman integrals as in Eq. (12.31),

$$W = A \left( \frac{k_B T}{\kappa} \right)^l \mu^{-2(l+v-1)} W^r, \quad (12.47)$$

where  $v$  is the number of vertices and  $l$  the number of lines of the diagram, we obtain

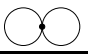
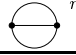
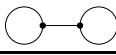
$$\Delta f_N = \alpha_N \frac{k_B^2 T^2}{\kappa a^2}, \quad (12.48)$$

$$\alpha_N = \frac{\pi^2}{N} \left( \frac{1}{4} \text{---} \text{---} \text{---} - \frac{1}{12} \text{---} \text{---} - \frac{1}{8} \text{---} \text{---} \right). \quad (12.49)$$

The pressure exerted by the membranes upon the walls is obtained by differentiating the free energy  $f_N = N \Delta f_N$  with respect to the distance of the walls  $L = a(N+1)$ :

$$p_N = -N \frac{\partial \Delta f_N}{\partial L} = \frac{2N}{N+1} \alpha_N \frac{k_B^2 T^2}{\kappa a^3}. \quad (12.50)$$

TABLE 12.2: Numeric values  $W^r$  of the reduced two-loop Feynman integrals contributing to the pressure constants of a stack of  $N$  membranes in Eq. (12.49).

$N$	 $r$	 $r$	 $r$
1	1/32	0	0
2	0.080542	0.022446	0.005582
3	0.131291	0.046992	0.009153
4	0.182239	0.071866	0.011529
5	0.233187	0.096762	0.013208
6	0.284099	0.121619	0.014453
7	0.334973	0.146428	0.015411
8	0.385815	0.171195	0.016172
9	0.436630	0.195925	0.016789
10	0.487422	0.220624	0.017300
11	0.538197	0.245300	0.017730
12	0.588958	0.269954	0.018097
13	0.639706	0.294592	0.018414
14	0.690444	0.319215	0.018690
15	0.741174	0.343827	0.018933

The first and the last Feynman integrals in Eq. (12.49) are the simplest:

$$\text{Figure-eight diagram} \equiv \frac{1}{32(N+1)^2} \sum_{n=1}^{N+1} \left[ \sum_{m=1}^N \frac{h_{nn}^m}{\sin(\nu_m a/2)} \right]^2, \quad (12.51)$$

$$\text{Two-circle diagram} \equiv \frac{1}{32(N+1)^3} \sum_{n_1, n_2=1}^{N+1} \sum_{\substack{m_1, m_2, \\ m_3=1}}^N \frac{h_{n_1 n_1}^{m_1} h_{n_1 n_2}^{m_2} h_{n_2 n_2}^{m_3}}{\sin(\nu_{m_1} a/2) \sin^2(\nu_{m_2} a/2) \sin(\nu_{m_3} a/2)}, \quad (12.52)$$

where we have used the abbreviation  $h_{n_1 n_2}^m$  defined in Eq. (12.30). The evaluation of the second diagram in Eq. (12.49) is much more involved. The Fourier integrals can be done exactly, except for one, which must be treated numerically. This calculation is deferred to Appendix 12A. The values of the three diagrams are listed in Table 12.2 for various numbers of membranes. With these numbers, the evaluation of the pressure constants yields the results given in Table 12.3. Except for  $N = 1$  and  $N \rightarrow \infty$ , no analytical values were found in the literature. We also compare with pressure constants obtained by Monte Carlo simulations and find a good agreement [86,88]. The values of the Monte Carlo simulations for  $N = 3, 5, 7$  from Ref. [86] show an independence of the number  $N$  of membranes. This arises by the simulation technique, where the free energy of the central membrane was determined. In contrast to that, we have calculated the pressure constant from the free energy of the complete system averaged over all membranes. Thus these Monte Carlo values cannot directly be compared with ours.

Table 12.3 contains also a value  $\alpha_\infty$  for an infinite number  $N \rightarrow \infty$  of membranes in the stack. This pressure constant is obtained by the following extrapolation procedure. We assume that the pressure constants determined for  $N = 12, 13, 14, 15$  are of higher accuracy than those for lower numbers of membranes. This assumption is justified by comparing our values for  $N = 1, 3, 5$  with the latest Monte Carlo results [88]. For  $N = 1$ , the deviation is about 3.4%. Considering  $N = 3$ , the deviation reduces to 1.8% and further to 1.1% for five membranes. Since the pressure constants are approximated increasingly fast with an increasing number  $N$  of membranes, we make the following exponential ansatz for determining the approach to infinite  $N$ :

$$\alpha_N = \alpha_\infty [1 - \eta \exp(-\xi N^\varepsilon)]. \quad (12.53)$$

The unknown four parameters in this equation are then determined by solving the system of equations with the pressure constants  $\alpha_{12}$ ,  $\alpha_{13}$ ,  $\alpha_{14}$ , and  $\alpha_{15}$  listed in Table 12.3. We obtain  $\eta \approx 1.1712$ ,

TABLE 12.3: Pressure constants  $\alpha_N$  for different numbers  $N$  of membranes in the stack, calculated from Eq. (12.49), with the numerical values of the two-loop diagrams given in Table 12.2. We compare with results from Monte Carlo simulations and earlier analytic results.

$N$	$\alpha_N$	Monte Carlo results	earlier analytic values
1	$\pi^2/128 \approx 0.07711$	0.060 [85], $0.078 \pm 0.001$ [86], $0.0798 \pm 0.0003$ [88], 0.080 [86]	$\pi^2/128$ [87,89], 0.079715 [48]
2	0.08669		
3	0.09134	$0.093 \pm 0.004$ [88], $0.1002 \pm 0.0006$ [86]	
4	0.09408		
5	0.09590	0.0966 [88], $0.1022 \pm 0.0006$ [86]	
6	0.09719		
7	0.09815	$0.1009 \pm 0.0007$ [86]	
8	0.09890		
9	0.09950		
10	0.09999		
11	0.10039		
12	0.10074		
13	0.10103		
14	0.10129		
15	0.10151		
$\infty$	0.10409	0.074 [104], $0.101 \pm 0.002$ [86], 0.106 [88]	$3\pi^2/128 \approx 0.23$ [50]

$\xi \approx 1.6417$ ,  $\varepsilon \approx 0.3154$ , and thus the limiting pressure constant for an infinite stack of membranes,

$$\alpha_\infty \approx 0.1041. \quad (12.54)$$

This value is in very good agreement with the Monte Carlo result [88] (see the last row of Table 12.3). It differs by a factor close to 9/4 from the initial result by Helfrich [50,105].

## 12A Evaluation of the Sunset Diagram

The second diagram in Eq. (12.49) requires some simplification before the numerical calculation. We write the reduced Feynman integral as

$$\textcircled{\text{---}}^r \equiv \frac{8}{A(N+1)^3} \sum_{n_1, n_2=1}^{N+1} \sum_{\substack{m_1, m_2, \\ m_3=1}}^N h_{n_1 n_2}^{m_1} h_{n_1 n_2}^{m_1} h_{n_1 n_2}^{m_1} K_{m_1 m_2 m_3} \quad (12A.1)$$

with the integral

$$K_{m_1 m_2 m_3} = \int d^2 x_1 d^2 x_2 \int \frac{d^2 k_1}{(2\pi)^2} \frac{d^2 k_2}{(2\pi)^2} \frac{d^2 k_3}{(2\pi)^2} \frac{e^{-i(\mathbf{k}_1 + \mathbf{k}_2 + \mathbf{k}_3)(\mathbf{x}_1 - \mathbf{x}_2)}}{(\mathbf{k}_1^4 + 2 \sin^2 \nu_{m_1} a)(\mathbf{k}_2^4 + 2 \sin^2 \nu_{m_2} a)(\mathbf{k}_3^4 + 2 \sin^2 \nu_{m_3} a)}. \quad (12A.2)$$

All integrals are easily calculated, except for one. If we introduce abbreviations

$$M_l^2 = 2 \sin^2 \nu_{m_l} a, \quad l = 1, 2, 3, \quad (12A.3)$$

we find

$$K_{m_1 m_2 m_3} = \frac{A}{2\pi} \int_0^\infty dk \frac{k}{\mathbf{k}^4 + M_3^2} J(\mathbf{k}, M_1^2, M_2^2) \quad (12A.4)$$

with

$$J(\mathbf{k}, M_1^2, M_2^2) = \int \frac{d^2p}{(2\pi)^2} \frac{1}{(\mathbf{p} - \mathbf{k})^4 + M_1^2} \frac{1}{\mathbf{p}^4 + M_2^2}. \quad (12A.5)$$

Decomposing the integrand into partial fractions

$$\begin{aligned} J(\mathbf{k}, M_1^2, M_2^2) &= -\frac{1}{4M_1M_2} \int \frac{d^2p}{(2\pi)^2} \left[ \frac{1}{(\mathbf{p} - \mathbf{k})^2 + iM_1} - \frac{1}{(\mathbf{p} - \mathbf{k})^2 - iM_1} \right] \left[ \frac{1}{\mathbf{p}^2 + iM_2} - \frac{1}{\mathbf{p}^2 - iM_2} \right] \\ &= -\frac{1}{4M_1M_2} [I(\mathbf{k}, M_1, M_2) - I(\mathbf{k}, M_1, -M_2) - I(\mathbf{k}, -M_1, M_2) + I(\mathbf{k}, -M_1, -M_2)], \end{aligned} \quad (12A.6)$$

we are left with integrals of the type

$$I(\mathbf{k}, \gamma_1, \gamma_2) = \int \frac{d^2p}{(2\pi)^2} \frac{1}{(\mathbf{p} - \mathbf{k})^2 + i\gamma_1} \frac{1}{\mathbf{p}^2 + i\gamma_2}, \quad (12A.7)$$

where  $\gamma_{1,2} = \pm M_{1,2}$  are real numbers. Employing Feynman's parameterization, these integrals become

$$I(\mathbf{k}, \gamma_1, \gamma_2) = \frac{1}{4\pi} \int_0^1 dx \frac{1}{-x^2k^2 + x(k^2 + i\gamma_1 - i\gamma_2) + i\gamma_2}, \quad (12A.8)$$

taking the general form

$$\int dx \frac{1}{ax^2 + bx + c} = \frac{2}{\sqrt{\Delta}} \arctan z(x) \quad (12A.9)$$

with

$$\Delta = 4ac - b^2, \quad z(x) = \frac{b + 2ax}{\sqrt{\Delta}}, \quad a = -k^2, \quad b = k^2 + i(\gamma_1 - \gamma_2), \quad c = i\gamma_2. \quad (12A.10)$$

Since  $b$  is a complex number,  $\text{Re} \arctan z$  is discontinuous, if  $\text{Re} z$  changes sign and  $|\text{Im} z| > 1$ . Thus the right-hand side of Eq. (12A.9) is discontinuous at a certain point  $x_0$  within the interval  $[0, 1]$ . As will be seen subsequently,  $J(\mathbf{k}, M_1^2, M_2^2)$  from Eq. (12A.5) must be real and thus all imaginary contributions in the decomposed form (12A.6) cancel each other.

We determine the point of discontinuity  $x_0$  to obtain the solution of the integral (12A.8) by investigating the zero of the real parts of  $z(x)$ . Decomposing  $z(x_0)$  into real and imaginary part, we obtain

$$\text{Re} z(x) = |\Delta|^{-1/2} \left[ k^2(1 - 2x) \cos \left( \frac{1}{2} \arctan \frac{\text{Re} \Delta}{\text{Im} \Delta} \right) + (\gamma_1 - \gamma_2) \sin \left( \frac{1}{2} \arctan \frac{\text{Re} \Delta}{\text{Im} \Delta} \right) \right], \quad (12A.11)$$

$$\text{Im} z(x) = |\Delta|^{-1/2} \left[ (\gamma_1 - \gamma_2) \cos \left( \frac{1}{2} \arctan \frac{\text{Re} \Delta}{\text{Im} \Delta} \right) - k^2(1 - 2x) \sin \left( \frac{1}{2} \arctan \frac{\text{Re} \Delta}{\text{Im} \Delta} \right) \right], \quad (12A.12)$$

where

$$\text{Re} \Delta = (\gamma_1 - \gamma_2)^2 - k^4, \quad \text{Im} \Delta = -2k^2(\gamma_1 + \gamma_2). \quad (12A.13)$$

Thus, the zero of  $\text{Re} z(x)$  is found at

$$x_0 = \frac{1}{2} \left\{ 1 + \frac{\gamma_1 - \gamma_2}{k^2} \tan \left[ \frac{1}{2} \arctan \frac{2k^2(\gamma_1 + \gamma_2)}{k^4 - (\gamma_1 - \gamma_2)^2} \right] \right\}. \quad (12A.14)$$

From the bounds of integration in Eq. (12A.8), it follows that we must include the discontinuities of Eq. (12A.9) for  $x_0 \in [0, 1]$ . This occurs if  $k < |\gamma_1 - \gamma_2|$  and  $\text{sign} \gamma_1 \neq \text{sign} \gamma_2$ . Thus the solution of the integral (12A.8) reads

$$I(\mathbf{k}, \gamma_1, \gamma_2) =$$

$$\left\{ \begin{array}{l} S(\mathbf{k}, \gamma_1, \gamma_2, x) \Big|_{x=0}^{x=1}, \quad \text{sign } \gamma_1 = \text{sign } \gamma_2 \vee (\text{sign } \gamma_1 \neq \text{sign } \gamma_2 \wedge k \geq \sqrt{|\gamma_1 - \gamma_2|}), \\ \lim_{\varepsilon \rightarrow 0} \left[ S(\mathbf{k}, \gamma_1, \gamma_2, x) \Big|_{x=0}^{x=x_0-\varepsilon} + S(\mathbf{k}, \gamma_1, \gamma_2, x) \Big|_{x=x_0+\varepsilon}^{x=1} \right], \quad \text{sign } \gamma_1 \neq \text{sign } \gamma_2 \wedge k < \sqrt{|\gamma_1 - \gamma_2|}, \end{array} \right. \quad (12A.15)$$

where  $S(\mathbf{k}, \gamma_1, \gamma_2, x)$  is the explicit right-hand side of Eq. (12A.9):

$$S(\mathbf{k}, \gamma_1, \gamma_2, x) = \frac{1}{2\pi\sqrt{(\gamma_1 - \gamma_2)^2 - k^4 - 2ik^2(\gamma_1 + \gamma_2)}} \arctan \frac{k^2(1 - 2x) + i(\gamma_1 - \gamma_2)}{\sqrt{(\gamma_1 - \gamma_2)^2 - k^4 - 2ik^2(\gamma_1 + \gamma_2)}}. \quad (12A.16)$$

The function  $I(\mathbf{k}, \gamma_1, \gamma_2)$  possesses the properties

$$I(\mathbf{k}, \gamma_1, -\gamma_2) + I(\mathbf{k}, -\gamma_1, \gamma_2) = 2\text{Re } I(\mathbf{k}, \pm\gamma_1, \mp\gamma_2), \quad (12A.17)$$

$$I(\mathbf{k}, \gamma_1, \gamma_2) + I(\mathbf{k}, -\gamma_1, -\gamma_2) = 2\text{Re } I(\mathbf{k}, \pm\gamma_1, \pm\gamma_2). \quad (12A.18)$$

Inserting Eq. (12A.15) into Eq. (12A.6), the remaining integral in Eq. (12A.4) together with the sums in expression (12A.1) for the sunset diagram can be calculated numerically. The values are listed for  $N = 1, \dots, 15$  in the third column of Table 12.2.

